Search for the electron electric dipole moment

D. DeMille*, S. Bickman*, P. Hamilton*, Y. Jiang*, V. Prasad*,
D. Kawall†, and R. Paolino‡

*Physics Department, Yale University, P.O. Box 208120, New Haven, CT 06520
†Physics Department, University of Massachusetts, Amherst, MA 01003
‡Science Department, U.S. Coast Guard Academy, New London, CT 06320

Abstract. Extensions to the Standard Model (SM) typically include new heavy particles and new mechanisms for CP violation. These underlying phenomena can give rise to electric dipole moments of the electron and other particles. Tabletop-scale experiments used to search for these effects are described. Present experiments are already sensitive to new physics at the TeV scale, and new methods could extend this range dramatically. Such experiments could be among the first to show evidence for physics beyond the SM.

Keywords: Electric dipole moments; CP violation; precision measurements.
PACS: 13.40.Em, 14.60.Cd, 32.80.Ys

EDMS, T-VIOLATION, AND THE SEARCH FOR NEW PHYSICS

An observable electric dipole moment (EDM) of any particle would be unambiguous evidence for physics beyond the Standard Model (SM) [1]. Moreover, in almost all viable extensions to the SM, EDMs are greatly enhanced compared to their SM values. Hence, the discovery potential of EDM searches is high.

The extreme sensitivity of EDMs to physics beyond the SM can be understood qualitatively. An EDM directed along the spin of a particle requires non-invariance under time-reversal (T). T-violation is incorporated in the SM via a complex phase in the CKM matrix. However, the SM is notable in that this is the *only* source of T-violation in the theory. This uniqueness leads to the very small predicted values of the EDMs in the SM. Consider e.g. the electron EDM, d_e. In the SM, a four-loop diagram is required to "access" the CKM phase and generate a non-zero d_e; moreover, there is a strong cancellation between diagrams (due to the GIM mechanism) [2].

By contrast, virtually every conceived extension of the SM includes new scalar fields, which allow new complex phases—and thus new sources of T-violation. The associated new particles generally induce a non-zero d_e at the two- or even one-loop level of perturbation theory, leading to a dramatically enhanced effect relative to the SM. It is difficult to justify any significant suppression of the new complex phases in such theories, for it is known that T is not even an *approximate* symmetry of nature: the T-violating phase in the CKM matrix is of order unity [3]. Moreover, it is generally accepted that the observed dominance of matter over antimatter in the universe actually requires *additional* sources of T-violation, beyond the CKM phase [4].

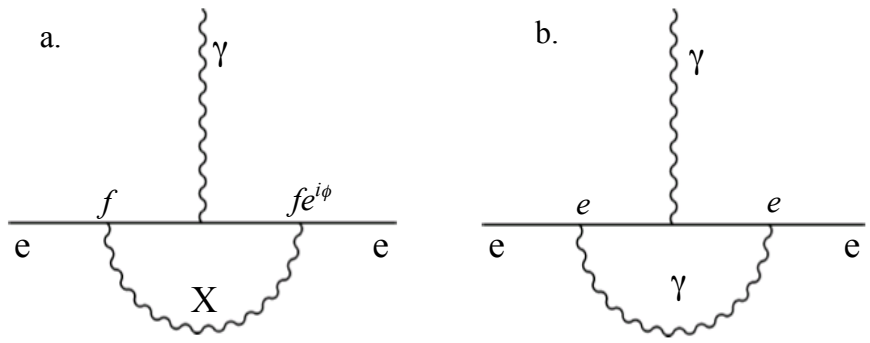

FIGURE 1. **a.** Generic one-loop diagram leading to an electron EDM. Note the CP-violating phase ϕ appearing at the vertex on the right side, and the loop involving the new particle, X, which couples to the electron with strength f. **b.** Diagram leading to electron g-2.

A crude quantitative argument makes it possible to estimate the value of d_e arising from a diagram of the type shown in Fig. 1a. Such a one-loop diagram is similar to that responsible for the magnetic anomaly of the electron, $(g\text{-}2)\mu_B \cong (\alpha/\pi)\mu_B$ (Fig. 1b). We can use this similarity to estimate d_e. The new features in the EDM diagram are: a) the heavy mass of the unknown virtual particle, m_X ; b) the inclusion of a CP-violating phase ϕ; and c) different couplings (f vs. e) at the vertices. The heavy-particle propagator introduces a factor of $1/m_X^2$ in the EDM diagram. Since m_e is the only other energy scale in the diagram, we expect on dimensional grounds that the dimensionless ratio of EDM to magnetic anomaly is $d_e/[(g\text{-}2)\mu_B] \propto (m_e/m_X)^2$. Thus $d_e \sim \sin\phi\ (f/e)^2\ (m_e/m_X)^2\ (\alpha/\pi)^2\ \mu_B$. In typical models, $\sin\phi \sim 1$ (just as in the CKM matrix), and the dimensionless ratio of coupling constants is $(f/e)^2 \sim 1$. For a typical one-loop diagram, this yields $d_e \sim 10^{-24}\ (100\ \text{GeV}/m_X)^2$ e·cm.

It is widely expected that new particles like X should have mass $m_X \sim 100$ GeV. This expectation arises from the "hierarchy problem": since the mass of the Higgs boson (m_H) is unstable to radiative corrections, "new physics" must appear near m_H in order to stabilize its value. Experimental constraints limit m_H to be in the range $114 < m_H < 200$ GeV [5,6]. Moreover, direct limits on the mass of new particles are frequently in the range ~100 GeV. Thus, one-loop diagrams can typically yield $d_e \sim 10^{-24}\,\text{e}\cdot\text{cm}$. In higher-order diagrams, each additional loop typically introduces a factor of order $\sim f^2/\pi \sim \alpha/\pi \sim 3\times10^{-3}$. Thus, it is natural that the current limit [7] $|d_e| < 1.6\times10^{-27}$ e·cm places severe constraints on theories where d_e appears at the one-loop level, and interesting constraints on theories where 2-loop diagrams are the leading order.

The most striking impact of EDM limits has been in the context of supersymmetry (SUSY). SUSY is widely accepted as a likely component of any viable theory for physics beyond the Standard Model [8]. One of the few recognized difficulties with SUSY is the observed smallness of EDMs.* EDMs appear in SUSY at the one-loop level, and hence the "natural" SUSY scale for d_e is $\sim10^{-25}$ e·cm—about 100× larger

* The current limits on d_e, d_n (the neutron EDM), and d_{Hg} (the EDM of the mercury atom) give broadly comparable limits on SUSY parameters, which vary somewhat in importance between specific models [9].

than the current limit! This "SUSY CP problem" is the subject of dozens of papers that discuss mechanisms to suppress EDMs below their natural scale in SUSY [9]. If d_e is not seen in the next few orders of magnitude—and if SUSY is correct—it becomes necessary to introduce fundamentally new theoretical constructions, as a means of suppressing CP violation in the mechanism of SUSY-breaking [10].

We have stressed above the importance of EDM constraints on SUSY models. However, recent reviews [11,12] emphasize that EDM limits impose severe constraints—typically stronger than from direct accelerator searches—on a much wider variety of models, which incorporate features such as left-right symmetry, multiple Higgs bosons, leptoquarks, composite fermions, etc. The situation is summarized in Fig. 2.

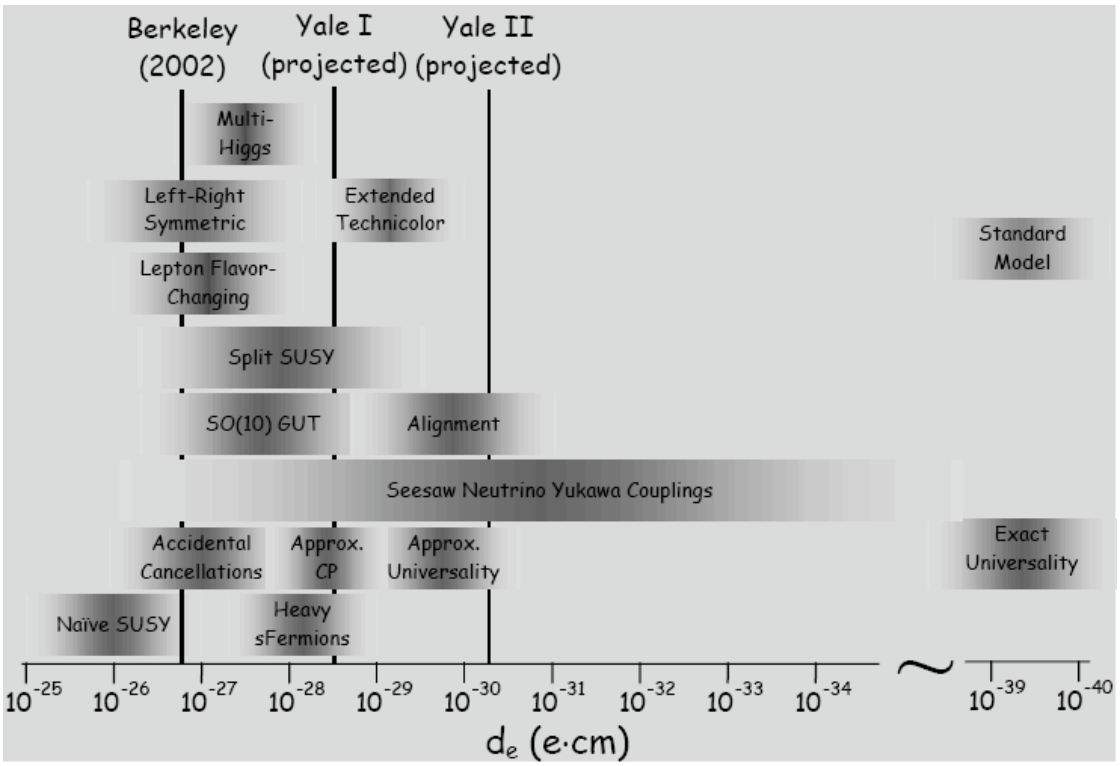

FIGURE 2. Impact of electron EDM limits. The x-axis indicates values for d_e. The vertical line "Berkeley (2002)" shows the current upper limit. Projected sensitivity from the first and second-generation search using PbO molecules at Yale also are shown. The shaded areas indicate predictions of specific models. The lowest five rows correspond to different variants of SUSY models. Note that the naïve predictions of SUSY are already ruled out. Note also the break in scale on the right of the plot: the SM prediction is roughly 13 orders of magnitude smaller than the current limit.

PRINCIPLES OF ELECTRON EDM SEARCHES

Any EDM experiment searches for a linear Stark shift ΔE arising from a term in the Hamiltonian of the form $H' = -d\vec{S}\cdot\vec{E}$, where $\vec{S}$ is the spin, $\vec{E}$ is an applied electric field, and $\vec{d} = d\vec{S}$ is the permanent EDM of the system [13]. In most experiments this is accomplished as follows. The spin $\vec{S}$ is initially aligned in a known direction,

typically via an optical pumping technique. For technical reasons, most experiments apply a magnetic field $\vec{B}$, perpendicular to $\vec{S}$. This creates a torque $\vec{\tau}_B = -\mu\vec{S}\times\vec{B}$ on the spin's magnetic moment $\vec{\mu} = \mu\vec{S}$, causing the spin to precess at frequency $\omega_B = \mu B/\hbar$. The electric field $\vec{E}$ is applied parallel to $\vec{B}$; hence the spin experiences an additional torque $\vec{\tau}_E = -d\vec{S}\times\vec{E}$, which slightly alters the precession frequency by an amount $\omega_E = dE/\hbar = \Delta E/\hbar$. The total precession frequency ◗ is monitored as the relative orientation of $\vec{E}$ and $\vec{B}$ is modulated: $\omega = \omega_B \pm \omega_E$, where the sign is the same as that for the T-odd invariant $\vec{E}\cdot\vec{B}$. The ultimate sensitivity of an EDM experiment depends both on the size of the frequency (or, equivalently, energy) shift, and the ability to accurately measure this small quantity. The energy resolution $\delta(\Delta E)$ can be parameterized simply: for shot-noise limited detection of a signal with a coherence time for an individual spin of τ, a counting rate of *dN/dt*, and a total integration time of *T*, the resolution is $\delta(\Delta E) = \hbar\Big/\left(\tau\sqrt{T\cdot(dN/dt)}\right)$.

For electron EDM experiments, understanding the size of the electric field E is a subtle matter. Naïvely, one might conclude that it is impossible to apply a large field to an electron, since it should accelerate rapidly out of the experiment due to the Coulomb force! However, the most sensitive searches for d_e use unpaired valence electrons, bound in neutral atoms or molecules. In this case, the Stark energy shift can be written as $\Delta E = d_e \cdot E_{eff}$, where E_{eff} is an effective internal electric field experienced by the valence electron(s). This effective field is nonzero only because of relativistic effects: essentially, the spin-orbit interaction leads to a magnetic force, which then allows a balancing electrostatic force inside the atom. This effect increases rapidly with atomic number *Z*; hence all EDM experiments use heavy atoms. The value of the effective field can be expressed as $E_{eff} = Q\Pi$, where Q is a factor which includes relativistic effects and the details of atomic structure, and Π is the polarization of the system induced by an external electric field $\vec{E}_{ext}$. Typical values (which depend on details of the electron wavefunctions) are [14] $Q \sim 5\times10^{10}$ V/cm $\times (Z/80)^3$.

Systematic effects are a primary concern in these experiments. The most dangerous systematics arise from spurious magnetic fields associated with application of $\vec{E}_{ext}$. These undesired fields can couple to $\vec{\mu}$, and result in systematic changes in the precession frequency that are correlated with the sign of $\vec{E}_{ext}$, much like the real EDM signal. Note that since for the electron $\mu_e \geq 10^{16} d_e$, even tiny effects can be important! A ubiquitous danger arises from magnetic fields generated by leakage currents associated with finite resistance across the electrodes used to generate $\vec{E}_{ext}$. More subtle effects—due e.g. to the motional magnetic field $\vec{B}_{mot} = \vec{E}_{ext}\times\vec{v}/c$ experienced by a particle moving at velocity $\vec{v}$ through the electric field—can also be extremely important. An ideal experiment incorporates a second "co-magnetometer" system, with a different value of μ/E_{eff}, to test for systematic effects.

RECENT AND ONGOING EXPERIMENTAL SEARCHES

The state-of-the-art electron EDM search was completed in 2002, in the group of E. Commins at Univ. of California, Berkeley [7]. This experiment used a thermal beam of Tl atoms (Z = 81, single valence electron). The 1 meter long beam resulted in a coherence time $\tau \sim 3$ ms. Alignment and detection of the spins was achieved via the Ramsey method of separated RF fields, with laser-induced optical pump and probe beams for spin alignment and readout. Application of a large field $\vec{E}_{ext} \cong 120$ kV/cm resulted in atomic polarization $\Pi \cong 10^{-3}$ and $E_{eff} \Psi 72$ MV/cm. The high-flux thermal beams and good detection efficiency led to large signal rates $dN/dt \Psi 1.7\times10^{9}$/s. Two parallel beams, in adjacent regions with equal but opposite values of $\vec{E}_{ext}$, were used to cancel noise due to residual drift and fluctuations in the magnitude of $\vec{B}$ (due e.g. to the local subway and nearby elevator), which was important despite the use of four layers of passive magnetic shields. This resulted in frequency measurements near the shot-noise limit. System instabilities limited the integration time to only $T \sim 35$ hr. Co-propagating beams of Na atoms (with Z = 11 and hence $\Theta \Psi 0$ and $E_{eff} \Psi 0$) were used as a co-magnetometer. Counter-propagating beams of both species were used to monitor and minimize motional field effects. The final quoted result, $|d_e| < 1.6\times10^{-27}$ e·cm (90% c.l.), includes roughly equal uncertainties from statistics and systematic errors.

There are currently at least nine new experiments attempting to reach improved sensitivity to d_e. (The Tl experiment reached its ultimate sensitivity and is no longer active.) These experiments are based on a remarkably wide variety of new techniques. Remarkably, most promise at least two, and as many as five, orders of magnitude improvement! These new experiments break generally into a few general types, which can be classified according to the key new technique as follows:

- Ultracold atoms. Here the primary motivation is to dramatically increase the coherence time ▼ through the use of slow-moving, laser-cooled atoms. Standard methods should allow excellent statistics. A drawback is that the heaviest convenient species is Cs (Z = 55), with a reduced value of Q and hence E_{eff}. Experiments are underway using atomic fountains [15] and optically-trapped atoms [16]. A lighter species such as Rb (Z = 37) can be used as a co-magnetometer. Up to a factor of 100 increase in sensitivity is anticipated.
- Solid-state systems [17]. The primary motivation is a dramatic increase in statistics associated with the high densities. The principle is rather different than outlined above; here the measured effect is not directly an energy shift, but rather a macroscopic property of the sample. For example, a paramagnetic solid will exhibit a small magnetization under the influence of an electric field, as the spins (and their magnetic moments) assume the energetically favored orientation of their EDMs. Possible systematic effects in these systems are not thoroughly understood at the moment. However, estimates of statistical sensitivity indicate that improvements of up to 10^5 may be possible, making these systems extremely promising nevertheless.

- Polar molecules. Here the primary motivation is a larger value of E_{eff}, associated with the ability to achieve electrical polarization $\mathcal{P} \cong 1$ using a modest external field. This increases the intrinsic sensitivity by a factor of 100-1000 [18]. The drawback of molecules is a loss of statistics due to the Boltzmann distribution over internal rotational states, and with the difficulty of producing paramagnetic (a.k.a. free radical) species. The first experiment of this type, using YbF molecules in a beam [19] is currently taking data and expects a small (<2) improvement in sensitivity over the Tl limit [20]. Our experiment, using PbO molecules in a vapor cell, will be described below. Other groups have begun exploring possibilities using cooled and trapped polar molecules to also achieve long coherence times [21]; however, these experiments will require significant technical advances in molecule cooling technology.

THE YALE PBO* EXPERIMENT

We are developing [22,23] an experiment to measure d_e using the paramagnetic metastable excited state *a(1)* [$^3\Sigma^+$, $|\Omega|=1$] of PbO [24]. This state has an effective field value $E_{eff} = 2\text{-}4\times10^{10}$ V/cm·$\mathcal{P}$ [25]. Use of PbO* makes it possible to perform the experiment in the high-density environment of a vapor cell rather than a beam, which leads to dramatically increased counting rates. The ability to work in a vapor cell arises only because several conditions can be simultaneously met. PbO (in its diamagnetic $X\ ^1\Sigma$ ground state) is thermodynamically and chemically stable; it is vaporized by heating to ~1000 K. The *a(1)* state can be efficiently populated by laser excitation, eliminating the need for free radicals. Finally, the *a(1)* state requires only small electric fields $E_{ext} \gtrsim 10$ V/cm to achieve $\mathcal{P} \approx 1$. The high polarizability of the *a(1)* state is a consequence of the small energy splitting (~12 MHz) between Ω-doublet opposite parity levels in this state [26]. The fairly long lifetime of the *a(1)* state ($\tau \approx 80$ μs [22]) also allows reasonable coherence times. These properties lead us to project an improved sensitivity to d_e by a factor of ~30 in the short term, and up to ~10^4 in the long term (with improved efficiencies of population and detection).

The basic technique for the EDM measurement is as follows. The measurement takes place in parallel static fields $E_{ext} \sim 50$ V/cm and $B \sim 0.05$ G. The eigenstates of the $m = \pm1$ components of the $J = 1$ Ω-doublet correspond to full polarization of the molecular axis, along or against $\vec{E}_{ext}$. (The $m = 0$ components are not mixed because the Clebsch-Gordan coefficient <1,0;1,0|1,0> vanishes.) The level diagram for this system is shown in Fig. 3.

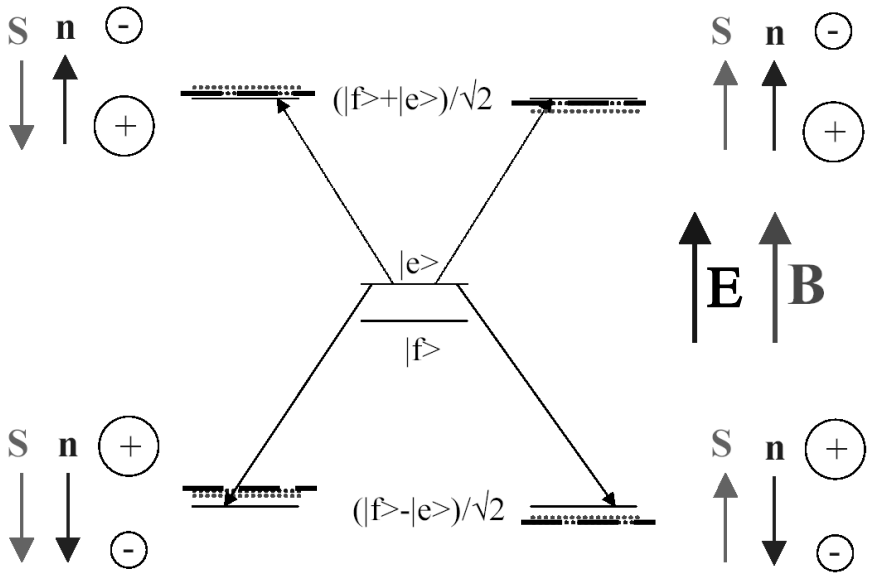

FIGURE 3. PbO* level structure with *E*- and *B*-fields. Only m = ±1 sublevels are polarized by E_{ext}. Vertical arrows labeled **S** and **n** indicate the direction of the spin and molecular axis (and hence $\vec{E}_{eff}$), respectively, of each polarized sublevel. Diagonal arrows indicate radiofrequency transitions from the laser-populated $|e, m = 0\rangle$ sublevel, which are used to populate a coherent superposition of $m = \pm 1$ for the EDM measurement. Dotted horizontal lines indicate the Zeeman splitting of sublevels; longer, dash-dotted horizontal lines indicate additional shifts due to d_e.

The $|J = 1^-, m = 0\rangle$ component of the *a(1)* state is selectively populated from the ground state, by a pulse of z-polarized laser light. Following the laser excitation pulse, a resonant radiofrequency pulse is used to transfer population from the $m = 0$ sublevel to a coherent superposition of the $m = \pm 1$ states, separated in energy from the $m = 0$ sublevel by □◗ with $\omega \sim$ 50-60 MHz typical. The superposition state has its spin vector aligned along the y-axis. It decays by emitting visible fluorescence in a dipole radiation pattern, with preferential emission in the direction parallel to the spin. Interaction with $\vec{B}$ and $\vec{E}_{eff}$ causes the $m = \pm 1$ components to acquire different phases, due to their different Zeeman and EDM shifts. This phase difference is equivalent to the precession angle of the spin alignment; it yields "quantum beats" (i.e., a sinusoidal amplitude modulation) in the fluorescence accompanying the decay of the *a(1)* state, at angular frequency ◗ = $2(g_p\mu_B B \pm d_e E_{eff})/$□. Here g_p is the effective *g*-factor of the polarized state, and μ_B is the Bohr magneton. The sign between the terms in the beat frequency is determined by the relative directions of the internal molecular electric field, $\vec{E}_{eff}$, and the magnetic field $\vec{B}$.

In addition, the PbO* system offers a new and powerful means for rejecting many systematic errors. Remarkably, the sign of E_{eff} can be changed *without* reversing $\vec{E}_{ext}$. Simply by changing the RF drive frequency by $\Delta_\Omega \cong$ 11.2 MHz (the field-free Ω-doublet splitting), we excite the other pair of nearly-degenerate $m = \pm 1$ levels, corresponding to a molecular polarization—and thus a sign of E_{eff}—opposite to the

original case (see Fig. 3). This additional reversal leads to dramatic reductions in potential systematic errors, because these oppositely-polarized levels respond almost identically to magnetic fields. The Ω-doublet levels of PbO may be thought of as an *internal* co-magnetometer. In the PbO system, the EDM energy shift can thus in principle be isolated by comparing the effect on the oppositely-polarized levels, *without the need to reverse* $\vec{E}_{ext}$. For d_e = 0, the difference of the beat frequency arising from the two polarized levels vanishes, even in the presence of spurious magnetic fields, to the extent that the g-factors of the polarized levels, g_{p+} and g_{p-}, are the same. Thus, requiring that the EDM signal reverse sign with a change of the internal value of E_{eff} (equivalent to the change between upward and downward diagonal arrows in Fig. 3), leads to a rejection of systematics due to spurious magnetic fields by a factor of $\sim g / \Delta g_p$, where $\Delta g_p = g_{p+} - g_{p-}$.

We recently completed set of experiments constituting a proof of concept for the electron EDM search using PbO* [27]. These experiments demonstrated most of the key features of the system, including:

- the ability to operate a vapor cell of PbO at the anticipated density, with collision-limited spin coherence time comparable to the spontaneous emission lifetime, in the presence of $\vec{E}_{ext}$ at the required level;
- the measurement of spin-precession frequencies with shot-noise limited uncertainty;
- the near equality of the g-factors of the polarized levels, indicating the possibility to suppress systematic effects by a factor of $g / \Delta g_p \approx 2000$.

We are now nearing the end of a long period of engineering improvements to optimize signal sizes and various elements of experimental control. This effort has resulted in the development of several novel techniques. For example, we designed and constructed different types of large-area, high-speed photodiode-based fluorescence detectors with fast recovery from transient overloads [28]. In addition, we found it necessary to implement the RF spin-flip pulses (shown in Fig. 3) using an indirect method. We drive a two-photon, stimulated Raman transition at microwave frequencies $f_\uparrow, f_\downarrow \approx 28.2$ GHz, resulting in population transfer up in energy to the $J = 2$ rotational level, then back down to the $J = 1$ level. Excitation with orthogonally-polarized microwave beams, with difference frequency $f_\uparrow - f_\downarrow$ at the desired RF transition frequency, results in population of the required superposition state. We anticipate taking our first EDM data shortly after submission of this manuscript, with projected sensitivity, after a few weeks of integration, at the level $d_e \approx 3\times10^{-29}$ e·cm.

ACKNOWLEDGMENTS

The PbO* work is supported by NSF Grant No. PHY0244927.

REFERENCES

1. See e.g. I.B. Khriplovich and S.K. Lamoreaux, *CP violation without strangeness: electric dipole moments of particles, atoms, and molecules*, Springer: New York, 1997.
2. M.E. Pospelov and I.B. Khriplovich, *Sov. J. Nucl. Phys*. **53**, 638 (1991).
3. A. Hocker *et al.*, *Eur. Phys. J. C* **21**, 225 (2001).
4. P. Huet and E. Sather, *Phys. Rev. D* **51**, 379 (1995).
5. W. Marciano, *Phys. Rev. D* **60**, 093006 (1999).
6. A. Raspereza, www.arxiv.org hep-ex/0209021.
7. B.Regan, E. Commins, C. Schmidt, and D. DeMille, *Phys. Rev. Lett.* **88**, 071805 (2002); E. Commins, S. Ross, D. DeMille, and B. Regan, *Phys. Rev. A* **50**, 2960 (1994); K. Abdullah, C. Carlberg, E. Commins, H. Gould, and S. Ross, *Phys. Rev. Lett.* **65**, 2347 (1990).
8. See e.g. G.L. Kane, in *Perspectives on Supersymmetry*, edited by G. Kane, World Scientific: Singapore, 1998, p. xv; F. Wilczek, *Int. J. Mod. Phys. A* **13**, 863 (1998); J.H. Schwarz and N. Seiberg, *Rev. Mod. Phys.* **71**, S112 (1999); J. Ellis, *Phys. World* **7**, 31 (1994).
9. For a recent review, see: S. Abel, S. Khalil, and O. Lebedev, *Nucl. Phys. B* **606**, 151 (2001).
10. We thank S. Barr for his summary of the recent theoretical trends regarding the CP problem in SUSY.
11. M. Suzuki, *Rev. Mod. Phys.* **63**, 313 (1991).
12. S. Barr, Int. *J. Mod. Phys. A* **8**, 209 (1993).
13. For a recent review, see N. Fortson, P. Sandars, and S. Barr, Phys. Today **56**, 33 (2003).
14. Calculated atomic enhancement factors ($R \equiv E_{eff}/E_{ext}$) and appropriate references are tabulated in Ref. [7].
15. J.M. Amini, C.T. Munger Jr., and H. Gould, www.arxiv.org physics/0602011.
16. D. Weiss (private communication); D. Heinzen (private communication).
17. S.K. Lamoreaux, *Phys. Rev. A* **66**, 022109 (2002); C.Y. Liu and S.K. Lamoreaux, *Mod. Phys. Lett. A* **19**, 1235 (2004); B.J. Heidenreich *et al., Phys. Rev. Lett.* **95**, 253004 (2005).
18. For a review of P- and T-odd effects in molecules, see M. Kozlov and L. Labzowsky, *J. Phys. B* **28**, 1933 (1995).
19. J.J. Hudson, B.E. Sauer, M.R. Tarbutt, and E.A. Hinds, *Phys. Rev. Lett.* **89**, 023003 (2002).
20. J.J. Hudson, B.E. Sauer, M.R. Tarbutt, and E.A. Hinds (private communication).
21. E. Cornell (private communication); N. Shafer-Ray (private communication).
22. D. DeMille, F. Bay, S. Bickman, D. Kawall, D. Krause, S. Maxwell, and L. Hunter, *Phys. Rev. A* **61**, 052507 (2000).
23. D. DeMille *et al*., in: *Art and Symmetry in Experimental Physics*, edited by D. Budker, P. Bucksbaum, and S. Freedman, AIP Conf. Proc. 596, Melville, New York, g2001, p. 72.
24. This was first suggested in: V. Flambaum, unpublished doctoral dissertation, Inst. of Nucl. Phys., Novosibirsk, Russia, 1987; see also: L. Barkov, M. Zolotorev, and D. Melik-Pashaev, *Sov. J. Quant. Electr.* **18**, 710 (1988).
25. There are two calculations of the internal electric field in PbO, which differ by a factor of ~2. See: M. Kozlov and D. DeMille, *Phys. Rev. Lett.* **89**, 133001 (2002), and A.N. Petrov *et al*., *Phys. Rev. A* **72**, 022505 (2005).
26. F. Martin *et. al.*, *Spectrochim. Acta* **44A**, 889 (1988).
27. D. Kawall, F. Bay, S. Bickman, Y. Jiang, and D. DeMille, *Phys. Rev. Lett.* **92**, 133007 (2004).
28. S. Bickman and D. DeMille, *Rev. Sci. Instrum*. **76**, 113101 (2005).